Applied Physics Letters

RESEARCH ARTICLE | MAY 10 2023

Interpretation of Josephson junction fluctuations at very low temperatures by superfluid flow equations

Special Collection: Electronic Noise: From Advanced Materials to Quantum Technologies

Chungho Cheng; Sergio Pagano ✉; Carlo Barone; ... et. al

Appl. Phys. Lett. 122, 192606 (2023)
https://doi.org/10.1063/5.0152369

AIP Publishing

Applied Physics Letters ARTICLE pubs.aip.org/aip/apl

Interpretation of Josephson junction fluctuations at very low temperatures by superfluid flow equations

Cite as: Appl. Phys. Lett. **122**, 192606 (2023); doi: 10.1063/5.0152369
Submitted: 29 March 2023 · Accepted: 27 April 2023 ·
Published Online: 10 May 2023

Chungho Cheng,[1] Sergio Pagano,[2,3,4,a)] Carlo Barone,[2,3,4] Niels Grønbech-Jensen,[1,5] Gaetano Salina,[6] James A. Blackburn,[7] and Matteo Cirillo[8]

AFFILIATIONS

[1]Department of Mechanical and Aerospace Engineering, University of California, Davis, California 95616, USA
[2]Dipartimento di Fisica "E. R. Caianiello," Università degli Studi di Salerno, 84084 Fisciano SA, Italy
[3]Istituto Nazionale di Fisica Nucleare, Gruppo Collegato Salerno, 84084 Fisciano SA, Italy
[4]CNR-SPIN, UOS Salerno, 84084 Fisciano SA, Italy
[5]Department of Mathematics, University of California, Davis, California 95616, USA
[6]Istituto Nazionale di Fisica Nucleare, Sezione di Roma Tor Vergata, 00133 Roma, Italy
[7]Department of Physics and Computer Science, Wilfrid Laurier University, Waterloo, Ontario N2L 3C5, Canada
[8]Dipartimento di Fisica and MINAS Lab, Università di Roma Tor Vergata, 00133 Roma, Italy

Note: This paper is part of the APL Special Collection on Electronic Noise: From Advanced Materials to Quantum Technologies.
[a)]**Author to whom correspondence should be addressed:** spagano@unisa.it

ABSTRACT

The effect of fluctuations on the stability of the zero-voltage state in the Josephson junction has been extensively investigated in the last four decades, due to the fundamental interest in this macroscopic quantum system and in view of possible application as a detector and, more recently, as base for quantum logic. Thermal induced escape from the zero-voltage state is well explained by consolidated theories based on the standard junction electrical model. However, at very low temperatures, significant deviations have been experimentally observed, which have triggered additional theories based on quantization of the Josephson junction effective potential and on macroscopic quantum tunneling. By looking at experiments carried out in the last forty years, we show here that the reported experimental data can be well described by standard theories down to zero temperature, provided that the Josephson potential is shifted by a constant amount, related to the junction plasma frequency. An explanation of this shift is given in terms of Anderson equations, relating chemical potential to phases, energies, and particle numbers in a superfluid flow.

Applications of weak superconductivity in several areas of cryogenic electronics and engineering[1–3] have stimulated work for characterizing noise phenomena in Josephson junctions and devices either from thermal[4] or from other physical sources.[5,6] Modeling based on the RCSJ (Resistively and Capacitively Shunted Junction)[7] electrical model has been very helpful in interpreting thermal fluctuations and escape phenomena in the Josephson effect.[8–10] Experimental data[11] on escape associated with fast bias current sweep have been framed within nonequilibrium dynamics[12] and specific initial conditions in the RCSJ model; these latter can also affect the escape process for high bias currents when temperature and dissipation are very low.[13] It has been recently shown that the Kramers model for thermal escape fails in describing the escape current distributions of the RCSJ model at very low temperatures and dissipation[10] while, in these limits, the Buttiker–Harris–Landauer (BHL)[9] model well describes the escape properties.

Both BHL and Kramers models, however, fail to describe relevant features observed in real experiments at very low temperatures on Josephson junctions. When the bias current becomes close to the junction critical current, the escape occurs for values lower than those predicted by the Kramers model (see, e.g., Ref. 14) and by the BHL as well.[10] This evidence suggests that the early escapes out of the

zero-voltage state, observed in the experiments for high values of the bias current, could be due to a sort of an "effective" lowering of the potential barrier responsible for the escape.

Within the RCSJ model, the energy of a single Josephson junction reads[16]

$$E(\varphi) = \frac{I_c \Phi_0}{2\pi}(1 - \cos\varphi) - \frac{I\,\Phi_0}{2\pi}\varphi. \tag{1}$$

In this equation, φ is the phase difference between the wavefunctions of the two superconductors generating the junction, I_c is the maximum Josephson supercurrent, I is the externally applied dc current, and $\Phi_0 = h/2e = 2.07 \times 10^{-15}$ Wb is the flux quantum ($h = 6.63 \times 10^{-34}$ J's is the Planck constant and $e = 1.60 \times 10^{-19}$ C is the electron charge). Normalizing Eq. (1) by the Josephson energy $E_j = \frac{I_c \Phi_0}{2\pi}$, we obtain the dimensionless potential:

$$U(\varphi) = (1 - \cos\varphi) - \eta\varphi, \tag{2}$$

where $\eta = I/I_c$ is the normalized bias current. From Eq. (2), it is possible to calculate, as a function of η, the "height" of the potential as the energy difference ΔU between a minimum and its successive maximum [see Fig. 1(a)]

$$\Delta U(\eta) = 2\left(\sqrt{1-\eta^2} - \eta\cos^{-1}\eta\right). \tag{3}$$

We recall now that, given a superfluid flow regulated by a phase parameter, just like by the phase difference between the electrodes of a Josephson junction φ, Anderson[16–18] predicted a relation between the time derivative of the phase parameter and the chemical potential μ in the form

$$\hbar\frac{d\varphi}{dt} = \frac{\partial E}{\partial N} = \mu \quad \text{or} \quad h\nu = \mu. \tag{4}$$

This equation, where $\hbar = h/2\pi$, holds for any frequency $\nu = \frac{\omega}{2\pi} = \frac{1}{2\pi}\frac{d\varphi}{dt}$ and expresses a dynamical process in which any deviation from the equilibrium is restored by the chemical potential, a condition which can generate eventually time oscillations of the phase. Indeed, if no voltages or external bias currents are applied this kind of oscillation is known as zero-bias Josephson plasma oscillations with a frequency $\upsilon_0 = \omega_0/2\pi = 1/2\pi\sqrt{\frac{2\pi I_c}{\Phi_0 C}}$,[7] where C represents the junction capacitance.

We associate to this frequency the corresponding energy and the "zero-bias" chemical potential, which we indicate as $h\nu_0 = \mu_0$. When applying the Kramers model to potential escape processes in the Josephson effect, the bias-dependent plasma frequency $\omega_j = \omega_0(1-\eta^2)^{\frac{1}{4}}$ plays a relevant role as an attempt frequency for the "jumps" out of the potential wells, Eq. (3), determining the escape rate $\Gamma(t)$ out of the potential itself, given by the equation[14]

$$\Gamma(t) = \omega_j \exp\left(-\frac{E_j \Delta U}{k_B T}\right), \tag{5}$$

where $k_B = 1.38 \times 10^{-23}$ J/K is the Boltzmann constant.

Based on the above considerations, even when $\eta = 0$ and the junction is in the zero-voltage state, an energy exists in the well, corresponding to the zero-bias current plasma oscillations, and its existence implies that the lowest energy attainable in the junctions will not be zero, corresponding to the minimum of $U(\varphi)$, but μ_0. Consequently, the effective height of the Josephson barrier, in the limit $T \to 0$, is obtained by replacing $E_j\Delta U$ with $(E_j\Delta U - \mu_0)$, with $\mu_0 = h\nu_0$. Therefore, the escape from the well will not occur for the maximum value $\eta = 1$ but for a slightly smaller value. Note that we are not modifying the shape of $U(\varphi)$, but we are shifting up the zero of the energy in Eq. (5) by a constant amount related to the zero-bias Josephson plasma frequency. The bias dependence of the phase oscillations in the potential well is considered in the attempt rate ω_j in Eq. (5).

The argument of the previous paragraph is consistent with two more equations derived by P. W. Anderson for superfluid flow.[17] One of these reads

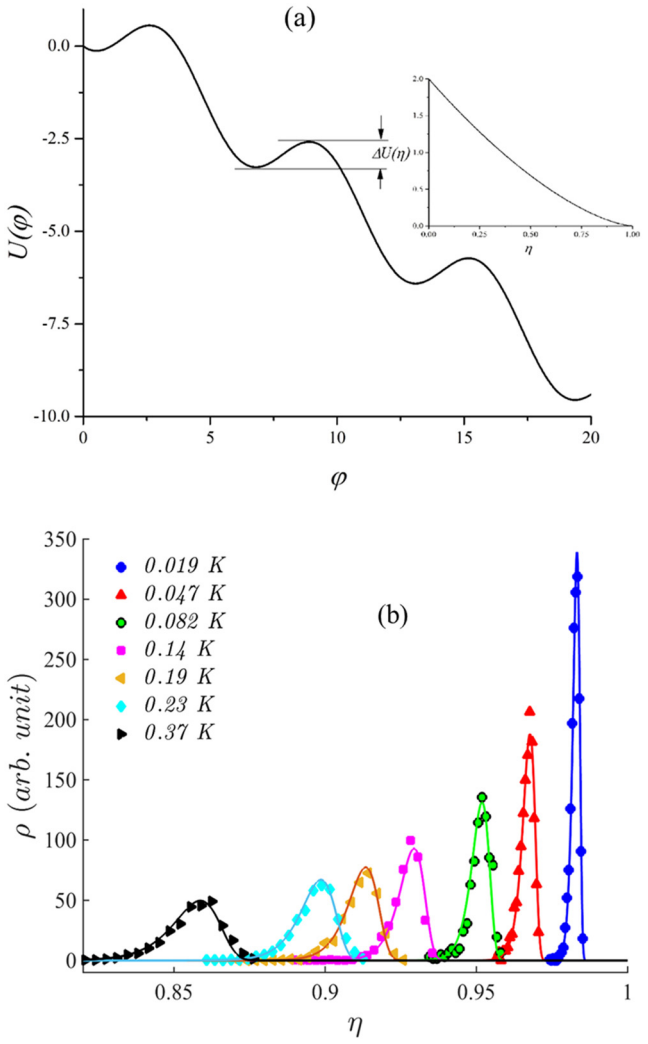

FIG. 1. (a) The Josephson potential $U(\varphi)$, from Eq. (2), for $\eta = 0.5$. The arrows indicate the barrier height ΔU. The inset shows the η dependence of ΔU. (b) Escape current distributions, obtained from numerical simulations of the RCSJ model with thermal fluctuations. The normalized bias sweep rate was 2.1×10^{-9}, the normalized dissipation was 0.05, and the Josephson critical current value was 1.957 μA (the same of Ref. 15). The solid curves represent the escape distributions computed by using Eq. (5) where ΔU is from Eq. (3).

$$\langle \mu_1 - \mu_2 \rangle = h \left\langle \frac{dN}{dt} \right\rangle \tag{6}$$

for the time averaged difference of the chemical potential generated by the presence of vortices between the two superfluid banks:[17] in that case, N represents the number of 2π advances due to vortices. In Josephson terms, the difference on the left side of Eq. (6) stands for an average chemical potential difference established by a voltage existing across the junction. The right-hand side stands for the time average of the time derivative of the number N of 2π phase advances, corresponding to a specific Josephson dc voltage across the junction. Equation (6) tells us that highest energy resolution would correspond to $N = 1$ (i.e., only one 2π phase-advance) when time is averaged in the shortest characteristic Josephson period (in dc voltage states Josephson phase advances in 2π increments). Taking as shortest Josephson time, the inverse of the zero-bias plasma frequency, Eq. (6) becomes $\langle \mu_1 - \mu_2 \rangle = h\nu_0 = \mu_0$, where we have averaged the right-hand side over $t = 1/\nu_0$ and assumed to have one 2π phase slip in this time. Thus, we find a limit resolution for the chemical potential (and voltage) difference to be possibly detected in characteristic time in the voltage state exists and this minimal resolution is established by μ_0.

A different way to look at the "quantum" limit discussed above comes from another Anderson equation, namely,

$$\hbar \frac{dn}{dt} = \frac{\partial E}{\partial \varphi}. \tag{7}$$

In this case, now n is the number of particles in the superfluid state (Cooper pairs of electrons). Assuming that $dn = 1$ as the minimal flow that could generate a 2π phase difference (and a dc voltage increase) across the junction, we find $\partial E\, dt = h$. Then, for the smallest possible variation of characteristic Josephson time $dt = 1/\nu_0$, we find that $\partial E = h\nu_0 = \mu_0$ is the minimal energy increment corresponding to a 2π phase flip generated the current flow of a single Cooper pair: We find again that it is reasonable to assume that the chemical potential μ_0 represents a limit for time-resolved energy detection processes in the Josephson effect.

In Fig. 1(b), we show some escape current distributions, obtained from numerical simulations of the RCSJ model in the presence of thermal fluctuations and by repeatably sweeping the bias current and recording the value of the current corresponding to the escape out of the zero-voltage state. Details of the integration routine are given in Refs. 13 and 14, Sec. 2.6. For comparison, in the same figure, the theoretical Kramers distributions, computed from Eq. (5) and using for ΔU the value from Eq. (3), are also shown as solid curves. We see that the peak position and the distribution width are well accounted for by the Kramers model down to tens of mK, in this case where the normalized dissipation is 0.05.[13] As recalled before, in the limit of very low temperatures (few hundreds of mK and below), and decreasing the dissipation, the distribution peak and width do not follow anymore the values expected from the Kramers theory and the BHL model is necessary to describe the escape features of the numerical simulations of the RCSJ model.[10]

However, both Kramers and BHL predict that, for "thermal" initial conditions of the system and when the temperature tends to zero, the distribution peak current should go to the unity, but this is not the case in the experiments where lower values are always observed.[15,19–27] Therefore, we can conclude that both Kramers and BHL models, and their related escape rate defined essentially by Eq. (5), can be adequate for the RCSJ dynamical system but do not describe real Josephson junctions escape features at very low temperatures.

We have extracted the values corresponding to the average escape current for the distributions, such as those shown in Fig. 1(b), from thermal escape measurements performed in the last four decades.[15,19–27] Such values have been compared with those obtained from the Kramers thermal escape Eq. (5) with $\Delta U_{\text{eff}} = \Delta U - \mu_0/E_j$ in place of ΔU, obtaining an average agreement (evaluated for all the considered experiments) contained within a 1.5% discrepancy. This remarkable agreement indicates that the experimental data, all taken in the tens of milliKelvin range, reach values close to the "zero-

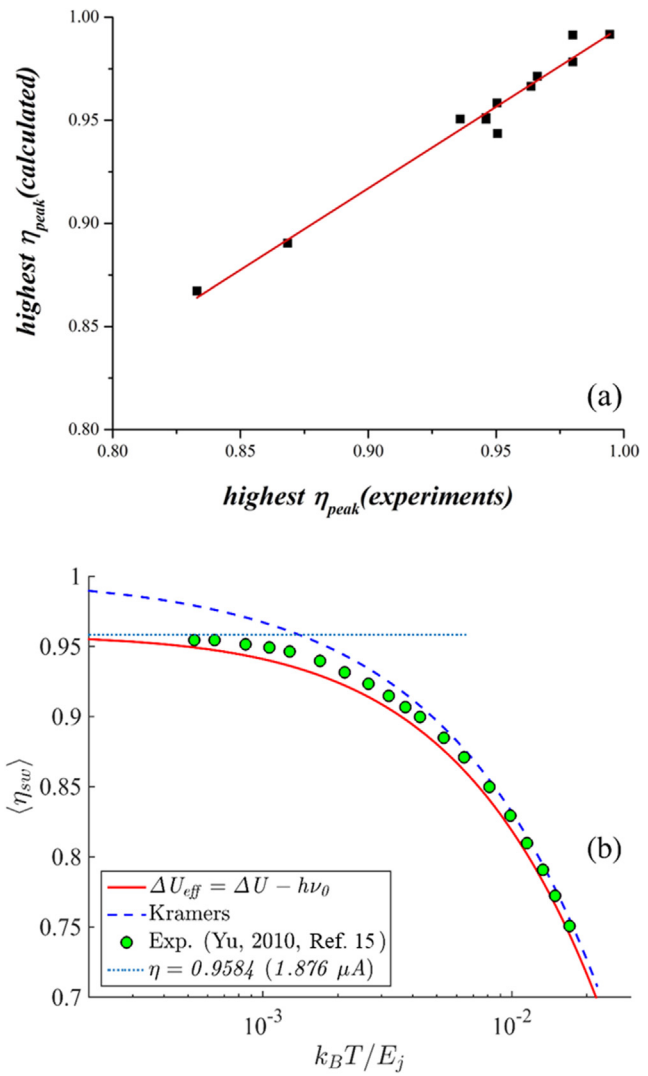

FIG. 2. (a) Comparison between the predictions of our model based on the limit set by the chemical potential μ_0: We have the experimental values on the horizontal axis and the "theoretical" predictions on the vertical axis. (b) The position of the escape peak taken from Ref. 15 compared with that obtained from escape simulations by subtracting to the Josephson potential the chemical potential.

temperature limit" already in this range. Thus, when the thermal energy $k_B T$ becomes comparable with μ_0, the effect of the chemical potential becomes significant.

In Fig. 2(a), we show a comparison between the proposed model and experiments. The plot is obtained recording on the horizontal axis the experimental values of the current corresponding to the peak of escape histograms, measured at the lowest reported temperatures, and on the vertical axis the corresponding value of our calculations based on the redefined potential barrier height. As we see the points are reasonably well aligned along a straight line (linear correlation coefficient 0.98, intercept 0.21 ± 0.06, and slope 0.78 ± 0.06). We note that the points are not aligned along with the bisector of the plane. This is not surprising since on the vertical axis we have values computed for $T = 0$ while on the horizontal axis we have experimental values measured in the tens of milliKelvin range. A statistical test (paired two sample t-test) performed to check the limits of the agreement gives a probability less than 10^{-5} that the predictions of our model and the experimental data are not related. The linear correlation shows that the chemical potential does have an effect in determining the limit values of the escape peaks.

In Fig. 2(b) are reported experimental data from Ref. 15 relative to the escape distribution peak position at different temperatures. The label of the vertical axis η_{sw} stands for switching current and represents the position, in normalized units, of the average current of the escape distributions. On the horizontal axis is reported the temperature normalized to E_j/k_B. These data are compared with Kramers and our proposed model. It is clearly shown that, when we use the μ_0 correction, the experimental data get closer to the theoretical curve in the very low temperature region, where the Kramers predictions deviate from the experimental data. We note that our model does not have any additional fitting parameter, and the value used for μ_0 is refereed to $T = 0$. Nevertheless, the good agreement with the experimental data is evident. In the figure legend is also reported the value of the extrapolated zero-temperature average escape current, in normalized units and in real units. The last value is computed using the junction critical current provided by Ref. 15.

Let us consider now the effect of non-zero temperature on the chemical potential. As custom in several contexts of thermodynamics and chemistry, we replace the value of the zero-temperature chemical potential $\mu_0 = h\nu_0$ by a simple expression generating its temperature

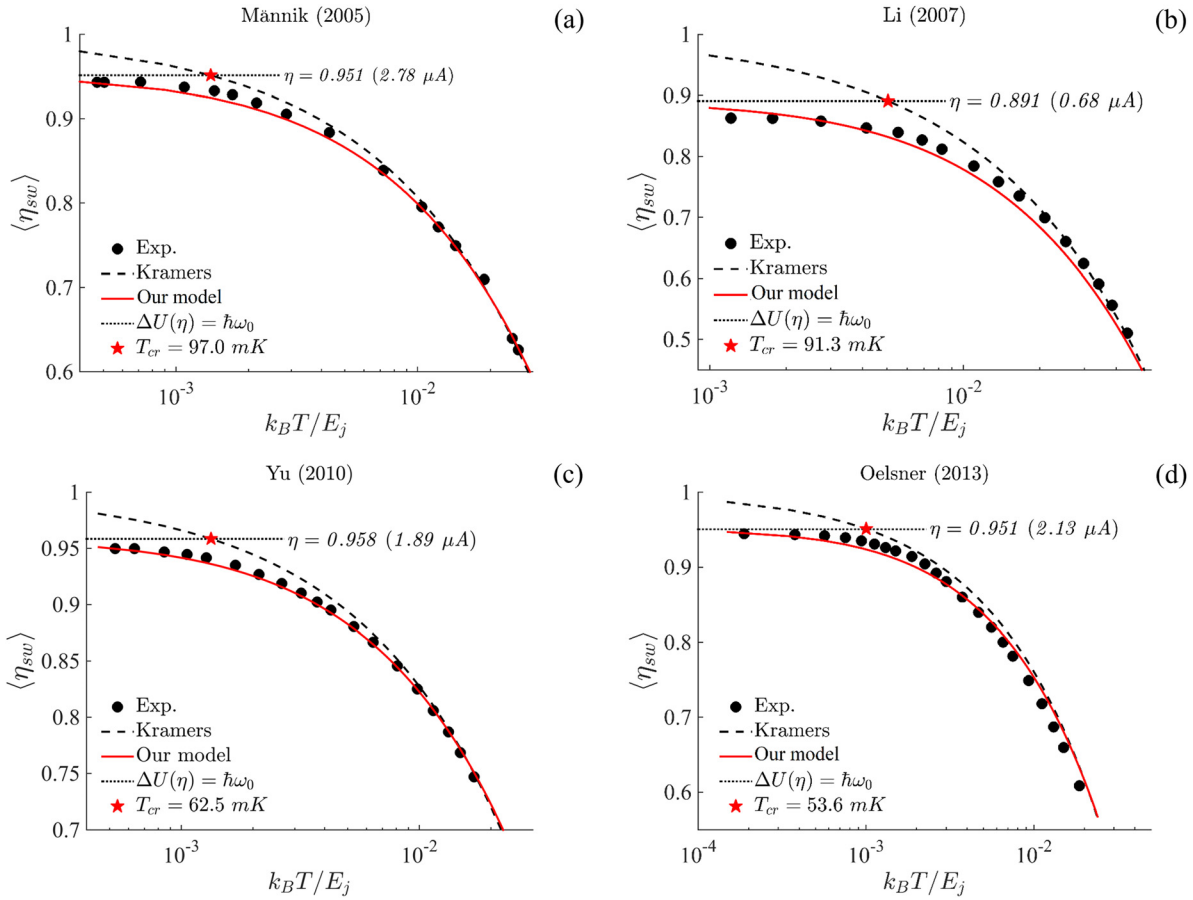

FIG. 3. The experimental results relative to the temperature dependence of the average switching current are shown along with the prediction of Kramers and our model in obtained for experiments reported in Refs. 26 (a), 23 (b), 15 (c), and 25 (d). Dots are experimental data, continuous lines show our model, and the dashed line is Kramers theory prediction. The horizontal dotted line represents the current value at which the effective energy barrier height vanishes, at $T = 0$ K. The intersection with Kramers prediction defines T_{cr}, identified by a star.

TABLE I. The main values extracted for the experiments and the results of the model presented here. I_c, C, dI/dt, and I_{sat} are derived from the experimental results reported in the work referred in the first column. I_{c_m} and I_{sat_m} are derived from the model presented here. $g = k_B/(h\nu_0)$, see main text.

Source	I_c (μA)	C (pF)	dI/dt (mA s^{-1})	I_{sat} (μA)	I_{c_m} (μA)	I_{sat_m} (μA)	g (K^{-1})
Männik *et al.*[26]	2.900	0.26	0.088	2.76	2.902	2.78	0.71
Li *et al.*[23]	0.748	0.088	0.16	0.66	0.796	0.68	0.81
Yu *et al.*[15]	1.957	0.62	0.4	1.86	1.967	1.89	1.34
Oelsner *et al.*[25]	2.200	0.33	0.0001	2.12	2.244	2.13	0.92

dependence. We choose the simple form $\mu(T) = \mu_0(1 - g\,T)$, where $\mu(T)$ is positive for T < 1/g and tends to μ_0 when $T \to 0$. Its effect becomes negligible for $T \geq 1/g$, and the escape rate of Eq. (5) returns to the standard Kramers expression. Here, g is a parameter giving the scale of temperature dependence of μ, and a reasonable assumption for its value is $g = k_B/\mu_0 = k_B/(h\,\nu_0)$. In this framework, we have compared with our improved model the available experimental data on the temperature dependence of the peak position of escape distribution histograms. In other terms, we replace now $E_j\,\Delta U$ in Eq. (5) with $E_j\,\Delta U - \mu(T)$, without introducing any fitting parameter.

Typical examples of such comparisons are shown in Fig. 3 in the case of the four experiments reported in Refs. 26 (a), 23 (b), 15 (c), and 25 (d). The dashed curve is the prediction of Kramers model, which overshoots the value of the critical current as the temperature approaches zero. The red continuous curve is the prediction of our model, which accounts also for the finite temperature, without additional fitting parameters. It is worth noting here that, in all experiments so far performed, the high-resolution value of the junction critical current is computed by fitting the experimental escape distribution data, taken at high temperatures with the Kramers model. Likewise, we have determined the junction critical current by fitting the experimental distribution data, taken at all temperatures, with our model. However, the difference is minimal and is shown in Table I for the cases referred in Fig. 3. In the same figure, the horizontal dotted line represents the current value at which the effective energy barrier height vanishes, at $T = 0$. The intersection with Kramers prediction defines T_{cr}, shown as a star symbol, which is useful to identify the range of temperatures below which Kramers model fails. The

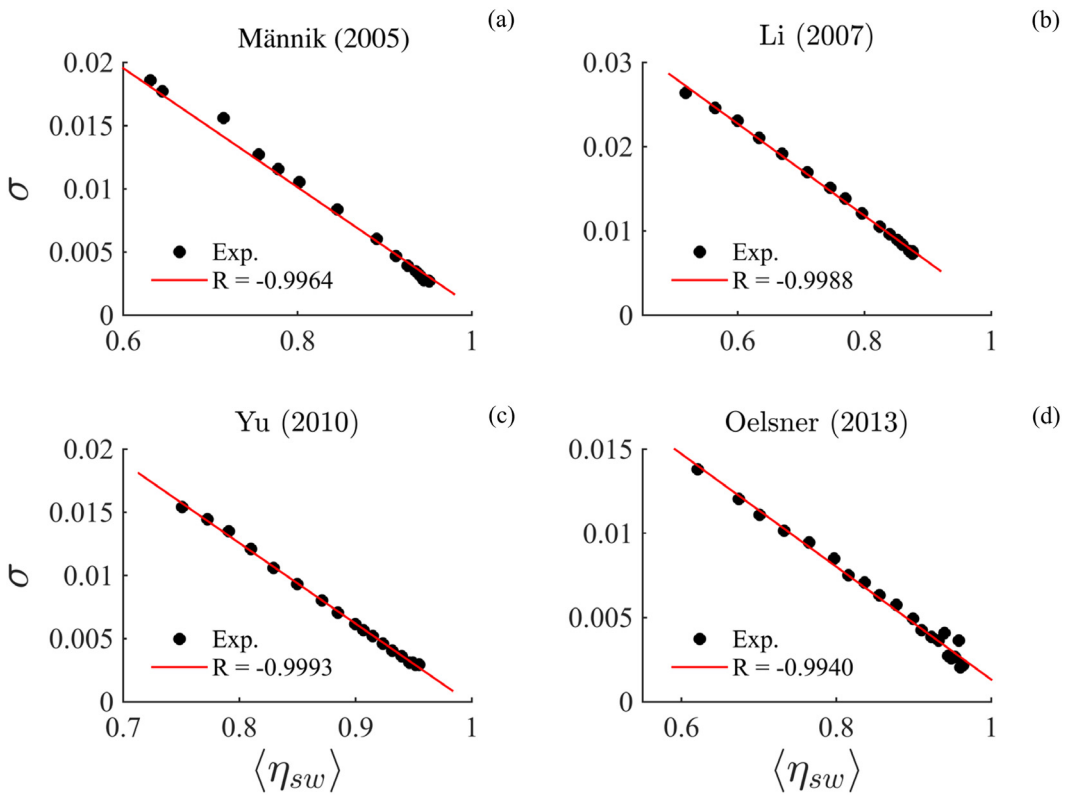

FIG. 4. Experimental distribution width vs average switching current, for each given temperature, as obtained from the experiments of Refs. 26 (a), 23 (b), 15 (c), and 25 (d). The R in the plot indicates the linear correlation coefficient. The linear dependence between these two parameters indicates the same functional dependence on temperature.

agreement between experimental data and our model is remarkable and represents a strong signature of the appropriateness of its physical basis.

In Table I are reported the experimental values of the junction parameters relative to four experiments reported in Refs. 15, 23, 25, and 26, and recalled in the first column. In the second column are the reported junction critical currents, obtained by the authors of the indicated papers as explained above from a fitting with the Kramers model in the high temperature range. The third column reports the junction capacitance as estimated in the experimental papers. The fourth column reports the slope of the current ramp used, while in the fifth column, the experimentally estimated zero-temperature saturation value of the average escape current is shown. In the sixth column, we show the values of the junction critical currents I_{c_m}, obtained by fitting the experimental data in the whole temperature range with our model for thermal escape. We note that this value is very close to that reported in the experimental papers, obtained, as discussed above, by fitting only the high temperature part of the escape current distributions. The seventh column shows the values of saturation currents, as derived from our model. The eightieth column reports the value of $g = k_B/(h\,\nu_0)$, computed using the evaluated critical current I_{c_m} and the junction capacitance, as declared in the experimental papers.

In Fig. 4, we now plot on one axis the average current position of the escape histogram and on the other axis the width of the histogram, relative to the same temperature, as extracted from the four sets of experimental data used in Fig. 3. As we see in the figure, the points on the plot are aligned along straight lines with linear correlation coefficients R very close to one, meaning that the two quantities on the axes have the same dependence on temperature. Note that the values of the bias current close to the unity will never be attained, as we have already discussed; plots very analogous to those shown in Fig. 4 were obtained for all the experiments we considered. The message of this plot is that, when analyzing escape processes in Josephson junctions, one can concentrate either on peak position or peak width since the two parameters identify each other.

As we see from Figs. 2 and 3, our modified Kramers escape rate produces very acceptable results for explaining the experimentally observed phenomena at very low temperatures on Josephson junction systems. Apart from the slight correction due to the chemical potential threshold, we see in Fig. 3 that the transition from "high" temperatures to the very low ones is smooth and there is no evidence of sharp phenomena, as should be expected, based on quantum escape,[28] for example, at the temperature marked by the red bar in Fig. 1 of Ref. 29. It is not surprising then that Josephson systems[14,30] can be modeled in several physical situations and circumstances (for example when weak rf pulses or rf signals are applied) by the classical RCSJ model.

We dedicate this endeavor to the memory of Professor Marc J. Feldman, outstanding investigator of superconductive quantum tunneling. His comments, and encouragement, at the early stages of the work leading to the results herein presented, were relevant.

S.P and C.B acknowledge financial support from University of Salerno, through Project Nos. FRB19PAGAN, FRB20BARON, FRB21CAVAL, and FRB22PAGAN, and from I.N.F.N. through projects SIMP, DARTWARS, and QUB-IT.

AUTHOR DECLARATIONS

Conflict of Interest

The authors have no conflicts to disclose.

Author Contributions

Chungho Cheng: Investigation (lead); Software (equal). **Sergio Pagano:** Conceptualization (equal); Writing – review & editing (lead). **Carlo Barone:** Validation (lead); Writing – review & editing (equal). **Niels Gronbech-Jensen:** Formal analysis (lead); Software (equal). **Gaetano Salina:** Conceptualization (equal); Software (lead). **James Blackburn:** Supervision (lead); Writing – review & editing (equal). **Matteo Cirillo:** Conceptualization (equal); Writing – original draft (lead).

DATA AVAILABILITY

The data that support the findings of this study are available from the corresponding author upon reasonable request.

REFERENCES

[1]A. Rettaroli, D. Alesini, D. Babusci *et al.*, Instruments **5**, 25 (2021).
[2]J. Ren and V. K. Semenov, IEEE Trans. Appl. Supercond. **21**, 780 (2011).
[3]N. P. de Leon, K. M. Itoh, D. Kim *et al.*, Science **372**, eabb2823 (2021).
[4]J. Kurkijärvi, Phys. Rev. B **6**, 832 (1972).
[5]R. F. Voss and R. A. Webb, Phys. Rev. B **24**, 7447 (1981).
[6]D. C. Cronemeyer, C. C. Chi, A. Davidson *et al.*, Phys. Rev. B **31**, 2667 (1985).
[7]A. Barone and G. Paternò, *Physics and Applications of the Josephson Effect* (John Wiley, New York, NY, 1982); also T. Van Duzer and C. W. Turner, *Principles of Superconductive Devices and Circuits* (Prentice Hall, Hoboken, NJ, 1999).
[8]H. A. Kramers, Physica **7**, 284 (1940).
[9]M. Büttiker, E. P. Harris, and R. Landauer, Phys. Rev. B **28**, 1268 (1983).
[10]C. Cheng, M. Cirillo, and N. Grønbech-Jensen, Entropy **23**, 1315 (2021).
[11]P. Silvestrini, V. G. Palmieri, B. Ruggiero *et al.*, Phys. Rev. Lett. **79**, 3046 (1997).
[12]C. Cheng, M. Cirillo, G. Salina *et al.*, Phys. Rev. E **98**, 012140 (2018).
[13]C. Cheng, G. Salina, N. Grønbech-Jensen *et al.*, J. Appl. Phys. **127**, 143901 (2020).
[14]J. A. Blackburn, M. Cirillo, and N. Grønbech-Jensen, Phys. Rep. **611**, 1–34 (2016).
[15]H. F. Yu, X. B. Zhu, Z. H. Peng *et al.*, Phys. Rev. B **81**, 144518 (2010).
[16]P. W. Anderson, "*Special effects in superconductivity*," in *Lectures on the Many Body Problem*, edited by E. R. Caianiello (Academic Press, New York, NY, 1964), Vol. 2, pp. 113–135.
[17]P. W. Anderson, Rev. Mod. Phys. **38**, 298 (1966).
[18]K. Huang, *Statistical Mechanics*, 2nd ed. (J. Wiley, New York, NY, 1987); see Sec. 13.6 on superfluid flow.
[19]R. F. Voss and R. A. Webb, Phys. Rev. Lett. **47**, 265 (1981).
[20]S. Washburn, R. A. Webb, R. F. Voss *et al.*, Phys. Rev. Lett. **54**, 2712 (1985).
[21]A. Wallraff, A. Lukashenko, C. Coqui *et al.*, Rev. Sci. Instrum. **74**, 3740 (2003).
[22]K. Inomata, S. Sato, K. Nakajima *et al.*, Phys. Rev. Lett. **95**, 107005 (2005).
[23]S.-X. Li, W. Qiu, S. Han *et al.*, Phys. Rev. Lett. **99**, 037002 (2007).
[24]H. F. Yu, X. B. Zhu, Z. H. Peng *et al.*, Phys. Rev. Lett. **107**, 067004 (2011).
[25]G. Oelsner, L. S. Revin, E. Il'ichev *et al.*, Appl. Phys. Lett. **103**, 142605 (2013).
[26]J. Männik, S. Li, W. Qiu *et al.*, Phys. Rev. B **71**, 220509(R) (2005).
[27]D. Massarotti, D. Stornaiuolo, P. Lucignano *et al.*, Phys. Rev. B **92**, 054501 (2015).
[28]J. M. Martinis and H. Grabert, Phys. Rev. B **38**, 2371 (1988).
[29]J. A. Blackburn, M. Cirillo, and N. Grønbech-Jensen, J. Appl. Phys. **122**, 133904 (2017).
[30]J. E. Marchese, M. Cirillo, and N. Grønbech-Jensen, Phys. Rev. B **79**, 094517 (2009).